A Density Functional Theory Based Approach to Extraframework Aluminum Species in Zeolites

Daniel L. Bhering,[†] Alejandro Ramírez-Solís,[‡] and Claudio J. A. Mota*[,†]

Departamento de Química Orgânica, Instituto de Química, Universidade Federal do Rio de Janeiro, Cidade Universitária CT Bloco A, 21949-900 Rio de Janeiro, Brazil, and Departamento de Física, Facultad de Ciencias, Universidad Autónoma del Estado de Morelos, Cuernavaca, Morelos 62210, Mexico

Received: October 30, 2002; In Final Form: January 30, 2003

The structures of six different extraframework aluminum (EFAL) species, possibly present in zeolites, were studied by density functional theory methods. A T_6 cluster (T = Si, Al), with different Si/Al ratios, was used to simulate the real zeolite Y structure and the coordination of the chosen EFAL species (Al^{3+}, $Al(OH)^{2+}$, AlO^{+}, $Al(OH)_2^{+}$, AlO(OH), and $Al(OH)_3$). The monovalent cations prefer to attain bicoordination with the framework AlO_4^{-} moiety, while di- and trivalent cations usually achieve tetracoordination. One important result is that, in all cases, coordination occurs with the oxygen atoms nearest to the framework aluminum ones. A single water molecule addition to the optimized $Al^{3+}\cdot T_6$ cluster produces a strongly exothermic reaction, leading to formation of a hydroxyaluminum cation and an acidic site on the zeolite. The addition of a second water molecule produces only minor energetic and structural changes.

Introduction

Zeolite-based acid catalysts are widely used in a number of commercially important petrochemical processes, including catalytic cracking, hydrocracking, and isomerization. Usually, chemical processes, to improve the physicochemical properties, catalytic activity, and thermal resistance,[1] are used to modify these catalysts. For zeolite Y, the principal component of cracking catalysts, steam dealumination is one of the main modification processes, among the many employed in the manufacture of these catalysts. It is normally conducted[2] by treating an ammonium-exchanged Y zeolite (with a framework Si/Al ratio around 2.5) with steam at temperatures ranging from 500 to approximately 700 °C. At these conditions the water molecules break the Al−O bonds, step by step, hypothetically releasing $Al(OH)_3$ out of the framework (Scheme 1). With longer reaction times and at high temperatures, the aluminum species released from the structure are transformed into a complex variety of species, which are mainly classified as condensed and noncondensed extraframework aluminum (EFAL). The structures of these EFAL species are not completely known, although some authors[3] quote the condensed species as Al_2O_3 phases, formed mostly at the external surface of the zeolite. The noncondensed species are normally associated with aluminum and oxyaluminum cations (AlO^{+}, $Al(OH)^{2+}$, Al^{3+}).[4] Dealumination increases the hydrothermal stability of the zeolites, which after this process are usually called ultrastable zeolites (USY). It also improves the catalytic performance in cracking, to produce high-octane gasoline. A dealuminated zeolite has the acid sites further away from each other, and in this way, they are less prone to undergo hydrogen transfer, giving less coke and a highly olefinic gasoline.[5]

The catalytic and acidic properties of dealuminated Y zeolites are a matter of great interest, from the theoretical as well as from the technological point of view. It is believed that EFAL species confer the Lewis acidity to the zeolites, since this kind of acid site normally appears after hydrothermal dealumination.[6] Yet, other dealumination methods, such as treatment with $(NH_4)_2SiF_6$, give an ultrastable Y zeolite free from EFAL species and mostly presenting only Brönsted acid sites.[7] The activity and selectivity of hydrocarbon conversion reactions are strongly influenced by EFAL species.[7] Guisnet and collaborators have studied[8] *n*-heptane cracking on USY zeolites, where part of the EFAL was leached by acid treatment. The results indicated that activity decreases as the amount of EFAL remaining in the zeolite is reduced. Lunsford and collaborators studied[9] the *n*-hexane cracking on USY zeolites, with and without EFAL species, as a function of the framework Si/Al ratio. They found that, regardless of the Si/Al ratio, the zeolites with EFAL showed a higher activity. Mota and collaborators[10] also found that the rate of H/D exchange of 3-methylpentane at 100 °C is about 20-fold higher, when EFAL is present in the USY zeolite.

SCHEME 1: Pictorial View of the Steam Dealumination Process of Zeolites

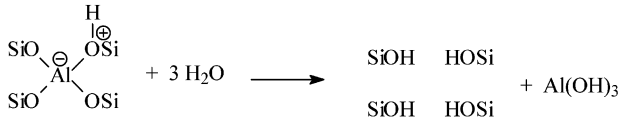

Most of the results of catalytic activity with USY zeolites having EFAL species were interpreted in terms of increasing the acid strength.[11] A synergistic effect between the Lewis and Brönsted acid sites is normally proposed (Chart 1).[12] Hence, the EFAL species (Lewis centers) interact with the electron pairs of the framework oxygen atoms, delocalizing the electron density near the Brönsted acid site, thus increasing acidity. This is sometimes referred to as a superacid site, since this kind of interaction is usually present in liquid superacid solutions.[13] Nevertheless, acidity measurements[14] indicated that zeolites cannot be considered real superacids, as their acid strengths are lower than that of 100% sulfuric acid. On the other hand, microcalorimety measurements with isopropylamine, pyridine,

[†] Universidade Federal do Rio de Janeiro.
[‡] Universidad Autónoma del Estado de Morelos.

10.1021/jp022331z CCC: $25.00
Published on Web 04/12/2003

CHART 1: Possible Superacid Site Formed by Interaction of EFAL Species with the Brönsted Acid Sites

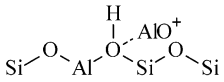

and ammonia revealed[15] that the presence of EFAL species in USY zeolites does not increase the acid strength, since the enthalpy of adsorption was rigorously the same for steam (with EFAL) and $(NH_4)_2SiF_6$ (without EFAL) dealuminated zeolites, with the same framework Si/Al ratio; these authors reported that a significant difference in catalytic activity was observed, with the zeolite presenting EFAL being about 10-fold more active for *n*-hexane cracking. However, no explanation for this behavior was presented. Indeed, this result suggests that EFAL structures may play a different role in changing the catalytic properties, rather than increasing the acid strength.

Another point of discussion is the role of the EFAL in abstracting a hydride from a hydrocarbon molecule to generate a carbocation. This pathway was proposed[16] more than 30 years ago to account for the initial carbenium ion formation in catalytic cracking.

Computational methods have been widely used in describing the structure, acidity, and catalytic performance of zeolites. Nevertheless, there are not many papers simulating EFAL structures of steamed zeolites. Benco et al. recently performed ab initio molecular dynamics calculations in some hydrated aluminum hydroxide inside zeolite channels.[17] Catlow and collaborators conducted a theoretical study on the defect formation upon zeolite dealumination.[18] Farcasiu and Lukinskas studied,[19] by density functional theory (DFT) methods, the structure of dialuminum oxide clusters, as models for EFAL species, and their role in H−H and C−H bond dissociation. Zhidomirov et al. also studied[20] the dialuminum oxide clusters, as models of EFAL and Lewis acid sites on zeolites. Ruiz and collaborators studied[21] the relative stability of tetracoordinated, pentacoordinated, and hexacoordinated aluminum hydroxy species, which can be considered as models of EFAL. The lack of theoretical studies for describing the structure and the catalytic activity of EFAL species in steam-dealuminated zeolites prompted us to carry out an investigation on this subject. We report here preliminary results concerning the structure of some EFAL species coordinated with a T_6 cluster.

Computational Details

To simulate the zeolite framework, a T_6 cluster (where T = Si or Al) was used (Figure 1), taking three different Si/Al ratios (3, 2, and 1), depending on the charge of the EFAL species studied. This cluster represents a real part of the zeolite Y structure, formed by two interconnected four-ring systems, one originally located in the hexagonal prism and the other in the sodalite cage, facing the supercage. Most of the hydrocarbon reaction occurs in the supercage, which has a pore opening of approximately 7.4 Å, while the sodalite cage has a pore opening of approximately 2.6 Å, being virtually inaccessible to the majority of the hydrocarbon molecules.

The silicon atoms on the edges were saturated with hydrogen atoms to avoid dangling bonds. Nevertheless, for all tetrahedral Al atoms of the framework, we used hydroxyl groups to complete the valence for a better description of the electron density near the aluminum atom. Six different species were chosen to simulate finite EFAL species, previously described in the literature: Al^{3+}, $Al(OH)^{2+}$, AlO^+, $Al(OH)_2^+$, AlO(OH), and $Al(OH)_3$. To compensate the charges, we included as many

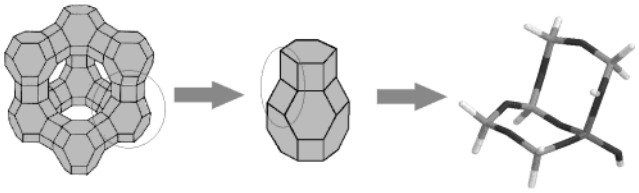

Figure 1. Structure of the T_6 cluster.

Al atoms as necessary in the cluster, to keep neutrality. This procedure may lead to a different Si/Al ratio in the cluster, but we are concerned with the study of the geometry and local coordination of the EFAL species, rather than measuring some thermodynamic property, such as acidity.

Calculations, within the DFT approximation, were performed to obtain minimum potential energy structures for the clusters modeled in this study. The harmonic frequency analysis was obtained using analytical second derivatives. Calculations were carried out with the Gaussian 98 package.[22] The DFT algorithm chosen combined Becke's three-parameter hybrid method, using the LYP correlation functional (B3LYP).[23] All the DFT calculations were performed using the Stevens, Basch, and Krauss effective core potentials (ECPs) and their associated valence basis functions.[24] To further enhance these basis sets, polarization and diffuse functions were added to all atoms. Details on the extended basis sets are available upon request from the authors.

The optimized structures were characterized as minima in the potential energy surface by the absence of imaginary vibrational frequencies. However, we do not claim that any of the structures presented here are the corresponding global potential energy minimum, especially for the larger EFAL species, since the number of spatial degrees of freedom is quite large. The vibrational frequencies, used to calculate zero-point energies (ZPEs), were scaled[25] by 0.96. Unless otherwise specified, all energies refer to the enthalpic term, corrected for ZPE and finite temperature at 298.15 K.

Results and Discussion

Structure of EFAL Species. Figure 2 shows the lowest energy optimized structures for the six different EFAL species studied in this work. It can be seen that in all cases the EFAL prefers to coordinate near the AlO_4^- tetrahedral moiety. The AlO^+ is symmetrically coordinated with the two oxygen atoms near the framework aluminum (structure **1a**). The Al−O distance of 1.85 Å in the coordination complex is about the same as the framework Al−O distance (1.87 Å). For structure **2**, representing the $Al(OH)_2^+$ coordinated with the T_6 cluster, the situation is similar. There is a preferential coordination of the EFAL species with the oxygen atoms near the framework aluminum. Again, the Al−O distances in the coordination complex and of the framework are about the same. It is interesting to note that the framework Al−O−Si bond angle (130.5°) is smaller than the Si−O−Si bond angle (141.7°), reflecting the coordination with the EFAL species. For the AlO^+ we were able to characterize two other minima in the potential energy surface; these EFALs were found to be tri- and tetracoordinated with the cluster (Figure 3). Structure **1b** reveals that the AlO^+ is tricoordinated with three AlO_4^- tetrahedra. This leads to a weaker coordination, reflected in the longer Al−O bond (1.91 Å), compared to the 1.86 Å for the Al−O distance in the framework. The tetracoordinated AlO^+ also has a weaker interaction with the framework, seen in the longer Al−O bond (around 2 Å) compared to the framework Al−O bond of 1.86 Å. The relative energy

TABLE 1: Valence Energies (hartrees), ZPEs, and Thermal Corrections for All the Calculated Structures

			B3LYP/ECP-31+G**			
structure	species	stoichiometry	*U* (hartrees)	ZPE (kcal/mol)	H_{298-0} (kcal/mol)	*S* (cal/(mol·K))
1a	AlO^+	$Al_2Si_5O_9H_{10}$	−174.04563	90.4	14.7	161.9
1b	AlO^+	$Al_2Si_5O_9H_{10}$	−174.0235	90.8	13.7	150.7
1c	AlO^+	$Al_2Si_5O_9H_{10}$	−174.02148	90.8	14.0	150.6
2	$Al(OH)^{2+}$	$Al_2Si_5O_{10}H_{12}$	−191.36894	99.0	15.2	162.5
3	AlO(OH)	$Al_2Si_5O_{10}H_{11}$	−190.78691	92.0	15.2	164.3
4	$Al(OH)_3$	$Al_2Si_5O_{11}H_{13}$	−208.07872	107.0	16.9	173.9
5a	$Al(OH)^{2+}$	$Al_3Si_4O_{11}H_{11}$	−204.97081	96.4	16.3	167.5
5b	$Al(OH)^{2+}$	$Al_3Si_4O_{11}H_{11}$	−204.95438	97.1	15.4	159.5
5c	$Al(OH)^{2+}$	$Al_3Si_4O_{11}H_{11}$	−204.96530	96.2	16.5	171.0
6	Al^{3+}	$Al_4Si_3O_{12}H_{10}$	−218.49312	92.9	16.6	171.5
7	$Al^{3+}\cdot T_6\cdot H_2O$	$Al_4Si_3O_{13}H_{12}$	−235.81209	110.5	17.8	174.4
8	$Al^{3+}\cdot T_6\cdot 2H_2O$	$Al_4Si_3O_{14}H_{14}$	−253.01472	125.4	19.6	189.5
	H_2O	H_2O	−17.18551	13.3	2.4	45.2

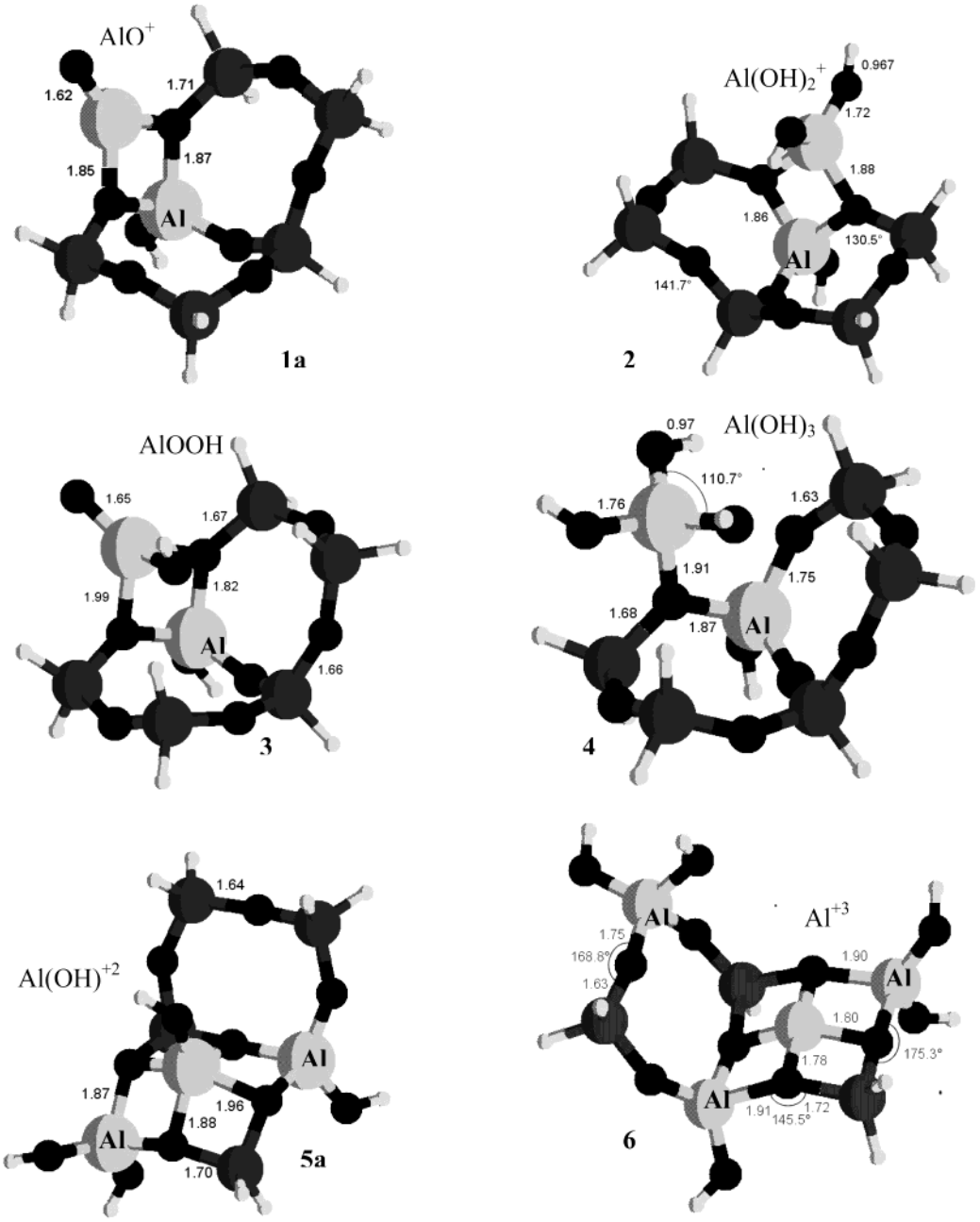

Figure 2. Optimized geometries of EFAL·T_6 at the B3LYP/ECP-31+G** level. Framework aluminum atoms are indicated (Al).

among structures **1a**, **1b**, and **1c** indicates that the bicoordinated AlO^+ (structure **1a**) is the most stable one. Structure **1b** lies 13.3 kcal/mol above **1a**, and structure **1c** is 14.9 kcal/mol higher in energy than **1a**. Both results are at the B3LYP-ECP-31+G**

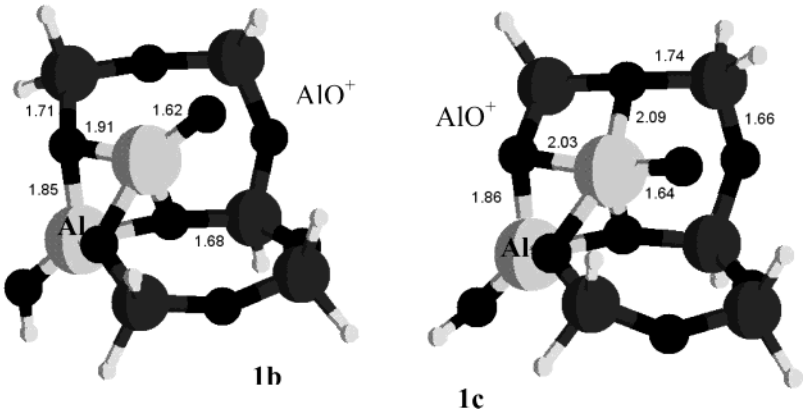

Figure 3. Other energy minima for $Al(OH)_2^+ \cdot T_6$ at the B3LYP/ECP-31+G** level. Framework aluminum atoms are indicated (Al).

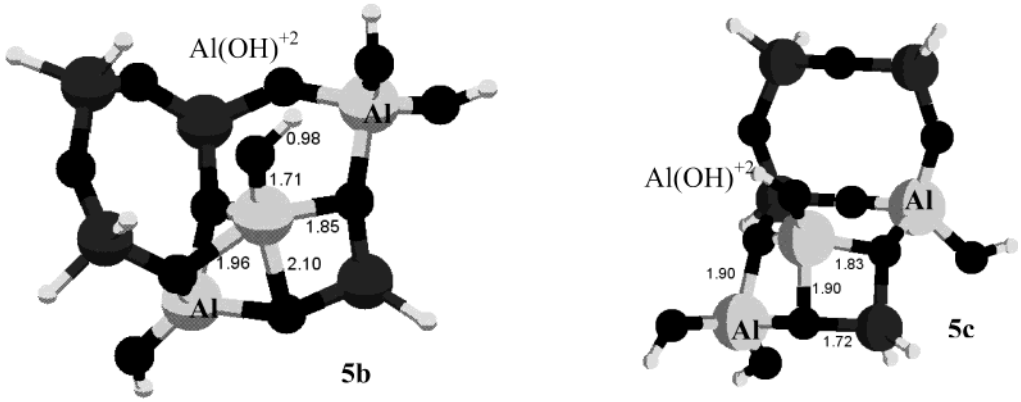

Figure 4. Other energy minima for $Al(OH)^{2+} \cdot T_6$ at the B3LYP/ECP-31+G** level. Framework aluminum atoms are indicated (Al).

TABLE 2: Relative Energies for the Different $Al(OH)_2^+ \cdot T_6$ and $Al(OH)^{2+} \cdot T_6$ Structures

		relative energy (kcal/mol)	
structure[a]	stoichiometry	B3LYP/ ECP-31+G**	B3LYP/ 6-311 +G**
1a	$Al_2Si_5O_9H_{10}$	0.0	0.0
1b	$Al_2Si_5O_9H_{10}$	13.3	12.6
1c	$Al_2Si_5O_9H_{10}$	14.9	15.4
5a	$Al_3Si_4O_{11}H_{11}$	0.0	
5b	$Al_3Si_4O_{11}H_{11}$	10.2	
5c	$Al_3Si_4O_{11}H_{11}$	3.5	

level. We decided to check the quality of the basis set used, by doing a single-point energy calculation at the B3LYP-6-311+G**/B3LYP-ECP-31+G** level. Table 2 shows the results, indicating that the difference between the two levels of calculation is within 1 kcal/mol, thus validating the use of the B3LYP/ECP-31+G** basis set to calculate the structure and energies of EFAL species.

For the neutral EFAL species studied in this work the situation is somewhat different. Structures **3** and **4** represent the coordination of AlOOH and $Al(OH)_3$ with the T_6 cluster, with one framework aluminum atom. It can be seen that the AlOOH prefers a coordination similar to those of the AlO^+ and $Al(OH)_2^+$ species, interacting with the two framework oxygen atoms near the Al site. However, the Al−O distances in the complex (1.99 Å) are longer than the framework Al−O distances (1.82 Å), indicating a weaker interaction, compared to the monovalent cations. This is due to the neutrality of the EFAL species, which requires less nucleophilic assistance from the framework. The $Al(OH)_3$ in structure **4** prefers a monocoordination with the framework, interacting only with one of the oxygen atoms. The extraframework aluminum atom attains a tetrahedral configuration, with angles near 110°, but the Al−O distance in the complex is longer (1.91 Å) than the framework Al−O bond (1.87 Å), also reflecting the weaker coordination with the framework, compared to the monovalent cations. This is again emphasized when one compares the Al−O bond in the EFAL moiety. The Al−O distance between the EFAL aluminum and the framework oxygen atom is 1.91 Å, which is significantly longer than the Al−OH bonds of 1.76 Å, found for the EFAL species.

Structure **5** shows the $Al(OH)^{2+}$ coordinated with the T_6 cluster, having two framework aluminum atoms. One can see that a tetracoordinated interaction with the framework is preferred, being located at about the center of the four-membered ring system having the two framework Al atoms. The $Al(OH)^{2+}$ cation is above the plane of the four-membered ring. The Al−O distances in the complex are 1.88 and 1.96 Å, while the Al−O bond distance in the framework is 1.87 Å. We also characterized two other stable minima for the $Al(OH)^{2+}$ species interacting with the T_6 cluster (Figure 4): another tetracoordinated one (**5b**) and one tricoordinated (**5c**). The main difference is that, in **5b** and **5c**, the $Al(OH)^{2+}$ cation is shifted toward one of the framework AlO_4^- anions. In **5b**, the $Al(OH)^{2+}$ coordinates with three oxygen atoms adjacent to the central framework Al. Structure **5c** resembles a distorted **5a**, where the EFAL species is moved away from the center of the four-membered ring toward one of the framework aluminums. Table 2 shows the relative energies among these structures, at the B3LYP/ECP-31+G** level of theory. The most stable structure is **5a**, having **5c** just 3.5 kcal/mol above. Structure **5b** is 10.2 kcal/mol higher in energy than **5a**.

Finally, we performed calculations for the Al^{3+} cation interacting with the T_6 cluster having three framework Al atoms. It can be seen that the Al^{3+} occupies the center of the four-membered ring, coordinating with the oxygen atoms near two

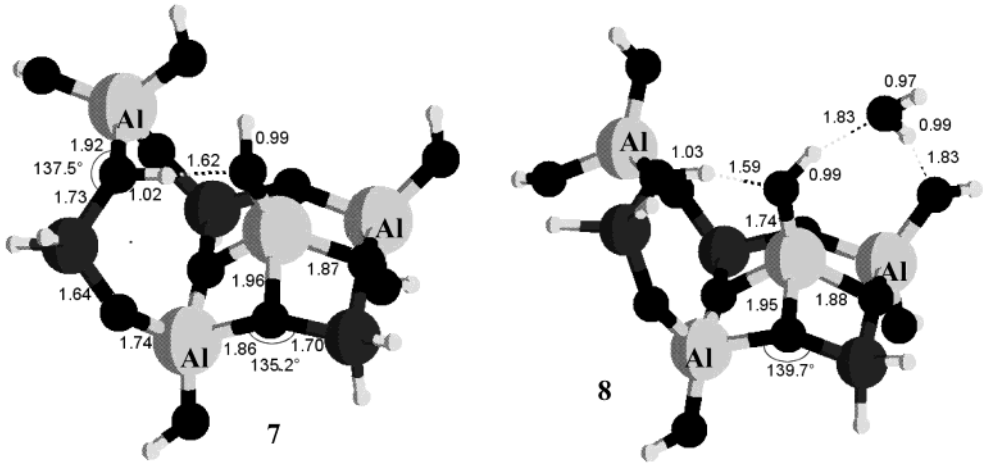

Figure 5. Optimized geometry for water reaction with $Al^{3+}\cdot T_6$ at the B3LYP/ECP-31+G** level. Framework aluminum atoms are indicated (Al).

TABLE 3: Thermodynamics for Water Reaction with the $Al^{3+}\cdot T_6$ Cluster, at the B3LYP/ECP-31+G Level**

reaction	ΔH (kcal/mol)	ΔS (cal/(mol·K))	ΔG^a (kcal/mol)
6 + $H_2O \rightarrow$ **7**	−79.1	−42.3	−66.5
7 + $H_2O \rightarrow$ **8**	−8.1	−30.1	+0.9

[a] $T = 298.15$ K.

framework aluminums only. It is interesting to note that the Al−O bond lengths of the complex are shorter (1.78 and 1.80 Å) than the framework Al−O bond near the cation (1.90 Å). The third framework Al atom, which is far from the Al^{3+} cation, shows a completely different geometry, with an Al−O bond length of 1.75 Å. This value is similar to the calculated Si−O bond length in the cluster (1.72 Å), showing that, in the absence of strong coordination, the AlO_4^- behaves similarly to the framework SiO_4.

Hydration of Al^{3+} EFAL. Zeolites are usually highly hygroscopic materials. The cations normally have a large affinity for adsorbing water molecules near their location. For instance, faujasite zeolites can take up to 25% of their weight in water. Yet, dealumination and EFAL formation are carried out under a water-rich atmosphere; therefore, subsequent interaction of the EFAL species with additional water molecules should be highly probable. To check this effect, we carried out calculations of structure **6**, Al^{3+} coordinated with the T_6 cluster, with one and two water molecules.

Table 3 shows the thermodynamics of water interaction with structure **6**. One can see that addition of the first water is strongly exothermic, releasing 79.1 kcal/mol of energy. Notwithstanding, the second water molecule releases only 8.1 kcal/mol. This is mostly canceled by the strong decrease in entropy (+30.1 cal/(mol·K)), overall making the Gibbs free energy slightly positive (+0.9 kcal/mol) at room temperature.

The strong exothermicity in the reaction of **6** with water can be explained by the structure of the product formed, **7** (Figure 5). The coordination of the water molecule with the Al^{3+} cation leads to a broken O−H bond in the water, forming a hydroxyaluminum complex and generating an acidic OH group on the framework. Also, as expected, the geometry of the cluster experiences a dramatic change upon water addition. For instance, the Al−O bond of the Al^{3+} complex increases from 1.78 and 1.8 Å in structure **6** to 1.96 and 1.87 Å after water addition (structure **7**). On the other hand, the framework Al−O bond length decreases from 1.91 Å in **6** to 1.86 Å in **7**. The Si−O−Al bond angle near the Al^{3+} also changes, from 145.5° to 135.2°. However, the greatest changes occur near the third framework aluminum atom. In structure **6** the Si−O−Al bond lengths and angle mostly resemble those of the Si−O−Si system. After water addition and formation of an acid site the Al−O bond length stretches from 1.75 Å in **6** to 1.92 Å in **7**. Yet the Si−O−Al bond angle shrinks from 168.8° in **6** to 137.5° in **7**, due to proton attachment in this oxygen atom. The acidic O−H bond is 1.02 Å long and makes a new hydrogen bond with the OH group coordinated to the aluminum cation. Addition of a second water molecule does not significantly alter the geometry (structure **8**). The additional water interacts with the hydroxyaluminum cation, forming hydrogen bonds with the cation and with the framework.

The fact that water addition to the EFAL generates an acidic site on the framework may indicate that different acid sites are formed on the framework, which may explain some of the experimental results. In fact, this kind of situation has long been proposed for rare-earth-metal-exchanged zeolites,[26] to explain their increased catalytic activity. Work is under way for studying the effect of EFAL on the acid strength and hydrocarbon activation.

Conclusion

The geometries of six different types of EFAL species coordinated to a T_6 cluster have been optimized at the B3LYP/ECP-6311+G** level of theory. For monovalent cations, such as AlO^+ and $Al(OH)_2^+$, a bicoordination with the oxygen atoms near the framework aluminum is the preferred structure. For di- and trivalent cations, tetracoordination is preferred, with the cationic EFAL occupying a position near the center of the four-membred ring containing two framework aluminum atoms.

Addition of one water molecule to the $Al^{3+}\cdot T_6$ cluster gives a strongly exothermic reaction, splitting the water O−H bond and leading to formation of a hydroxyaluminum cation plus an acid site on the framework.

Acknowledgment. C.J.A.M. thanks PRONEX, CNPq, FAPERJ, and CTPETRO for financial support. D.L.B. is grateful to the National Petroleum Agency for a doctoral scholarship (PRH-ANP). A.R.S. acknowledges partial support from CONACYT (Mexico) through Project No. 34673-E.

References and Notes

(1) (a) Cusumano, J. A. In *Perspectives in catalysis*; Thomas, J. M., Zamaraev, K. I., Eds.; Blackwell Scientific Publication: Boston, 1992. (b) Pines, H. In *The Chemistry of Catalytic Hydrocarbon Conversion*; Academic Press: New York, 1981.

(2) (a) Wang, Q. L.; Giannetto, G.; Torrealba, M.; Perot, G.; Kappenstein, C.; Guisnet, G. *J. Catal.* **1990**, *130*, 459. (b) Guisnet, M.; Wang, Q. L.; Giannetto, G. *Catal. Lett.* **1990**, *4*, 299.

(3) (a) Shannon, R. D.; Gardner, K. H.; Staley, R. H.; Bergeret, G.; Gallezot, P.; Arnoux, A. *J. Phys. Chem.* **1985**, *89*, 4778. (b) Remy, M. J.; Stanica, D.; Poncelet, G.; Feijen, E. J. P.; Grobet, P. *J. Phys. Chem.* **1996**, *100*, 12440.

(4) Scherzer, J. *ACS Symp. Ser.* **1984**, *248*, 157.

(5) (a) Pine, L. A.; Maher, P. J.; Wachter, W. A. *J. Catal.* **1984**, *85*, 466. (b) Habib, E. T., Jr. In *The Hydrocarbon Chemistry of FCC Naphtha Formation*; Lovink, H. J., Pine, L. A., Eds.; Technip: Paris, 1990; p 1.

(6) (a) Jacobs, P. A.; Beyer, H. K. *J. Phys. Chem.* **1979**, *83*, 1174. (b) Datka, J. *J. Chem. Soc., Faraday Trans. 1* **1981**, *77*, 2877. (c) Catana, G.; Baetens, D.; Mommaerts, T.; Schoonheydt, R. A.; Weckhuysen, B. M. *J. Phys. Chem. B* **2001**, *105*, 4904.

(7) (a) Fleisch, T. H.; Meyers, B. L.; Ray, G. J.; Hall, J. B.; Marshall, C. L. *J. Catal.* **1986**, *118*, 85. (b) Kuehne, M. A.; Kung, H. H.; Miller, J. T. *J. Catal.* **1997**, *171*, 293.

(8) Wang, Q. L.; Giannetto, G.; Guisnet, G. *J. Catal.* **1991**, *130*, 471.

(9) Carvajal, R.; Chu, P. J.; Lunsford, J. H. *J. Catal.* **1990**, *125*, 121.

(10) Mota, C. J. A.; Martins, R. L.; Nogueira, L.; Kover, W. B. *J. Chem. Soc., Farady Trans.* **1994**, *90*, 227.

(11) (a) Fritz, P. O.; Lunsford, J. H. *J. Catal.* **1989**, *118*, 85. (b) Beran, S. *J. Phys. Chem.* **1990**, *94*, 335. (c) Lónyi, F.; Lunsford, J. H. *J. Catal.* **1992**, *136*, 566.

(12) Corma, A.; Fornés, V.; Rey, F. *Appl. Catal.* **1990**, *59*, 267.

(13) Olah, G. A.; Prakash, G. K. S.; Sommer, J. In *Superacids*; Wiley: New York, 1985.

(14) (a) Umansky, B. S.; Hall, W. K. *J. Catal.* **1990**, *124*, 97. (b) Umansky, B. S.; Engelhadt, J.; Hall, W. K. *J. Catal.* **1990**, *127*, 128. (c) Xu, T.; Munson, E.; Haw, J. *J. Am. Chem. Soc.* **1994**, *116*, 1962.

(15) (a) Biaglow, A. I.; Parrillo, D. J.; Kokotailo, G. T.; Gorte, R. J. *J. Catal.* **1994**, *148* (1), 213. (b) Beyerlein, R. A.; Choi-Feng, C.; Hall, J. B.; Huggins, B. J.; Ray, G. J. *Top. Catal.* **1997**, *4* (1−2), 27.

(16) (a) Tung, S. E.; McInich, E. *J. Catal.* **1968**, *10*, 166. (b) Nace, D. M. *Ind. Eng. Chem. Prod. Res. Dev.* **1980**, *58*, 219. (c) Borodzinski, A.; Corma, A.; Wojciechowski, B. W. *Can. J. Chem. Eng.* **1980**, *58*, 219.

(17) Benco, L.; Demuth, T.; Hafner, J.; Hutschka, F.; Toulhoat, H. *J. Catal.* **2002**, *209*, 480.

(18) (a) Sokol, A. A.; Catlow, C. R. A.; Garcés, J. M.; Kuperman, A. *Adv. Mater.* **2000**, *12*, 1801. (b) Sokol, A. A.; Catlow, C. R. A.; Garcés, J. M.; Kuperman, A. *J. Phys. Chem. B* **2002**, *106*, 6163.

(19) (a) Lukinskas, P.; Farcasiu, D. *Appl. Catal., A* **2001**, *209*, 193. (b) Farcasiu, D.; Lukinskas, P. *J. Phys. Chem.* **2002**, *106*, 1619.

(20) Zhidomirov, G. M.; Yakovlev, A. L.; Milov, M. A.; Kachurovskaya, N. A.; Yudanov, I. V. *Catal. Today* **1999**, *51*, 397.

(21) Ruiz, J. M.; McAdon, M. H.; Garcés, J. M. *J. Phys. Chem. B* **1997**, *101*, 1733.

(22) Frisch, M. J.; Trucks, G. W.; Schlegel, H. B.; Scuseria, G. E.; Robb, M. A.; Cheeseman, J. R.; Zakrzewski, V. G.; Montgomery, J. A., Jr.; Stratmann, R. E.; Burant, J. C.; Dapprich, S.; Millam, J. M.; Daniels, A. D.; Kudin, K. N.; Strain, M. C.; Farkas, O.; Tomasi, J.; Barone, V.; Cossi, M.; Cammi, R.; Mennucci, B.; Pomelli, C.; Adamo, C.; Clifford, S.; Ochterski, J.; Petersson, G. A.; Ayala, P. Y.; Cui, Q.; Morokuma, K.; Malick, D. K.; Rabuck, A. D.; Raghavachari, K.; Foresman, J. B.; Cioslowski, J.; Ortiz, J. V.; Stefanov, B. B.; Liu, G.; Liashenko, A.; Piskorz, P.; Komaromi, I.; Gomperts, R.; Martin, R. L.; Fox, D. J.; Keith, T.; Al-Laham, M. A.; Peng, C. Y.; Nanayakkara, A.; Gonzalez, C.; Challacombe, M.; Gill, P. M. W.; Johnson, B. G.; Chen, W.; Wong, M. W.; Andres, J. L.; Head-Gordon, M.; Replogle, E. S.; Pople, J. A. *Gaussian 98*, revision A.7; Gaussian, Inc.: Pittsburgh, PA, 1998.

(23) (a) Lee, W. Y.; Parr, R. G. *Phys. Rev. B* **1988**, *37*, 785. (b) Becke, A. D. *Phys. Rev. A* **1988**, *38*, 3098.

(24) (a) Stevens, W. J.; Basch, H.; Krauss, M. *J. Chem. Phys.* **1984**, *81*, 6026. (b) Stevens, W. J.; Krauss, M.; Basch, H.; Jasien, P. G. *Can. J. Chem.* **1992**, *70*, 612.

(25) Hehre, W. J.; Radom, L.; Schleyer, P. V. R.; Pople, J. In *Ab initio Molecular Orbital Theory*; Wiley: New York, 1986.

(26) (a) Ward, J. W. *Zeolite Chem. Catal., ACS Monogr.* **1976**, *171*, 118. (b) Marynem, P.; Maes, A.; Cremers, A. *Zeolites* **1984**, *4*, 287. (c) Keir, D.; Lee, E. F. T.; Rees, L. V. C. *Zeolites* **1988**, *8*, 228.